Volume 8 No. 1 Oct. - Dec. (1-71) 1994
J. Laser Sci. & Tec., Vol. 8, No. 1, 24-42 (1994)

NEW OPPORTUNITIES IN INFRARED LASER SPECTROSCOPY

F.K. Tittel

Department of Electrical and Computer Engineering
Rice University, P.O.Box 1892, Houston, Texas 77251

Received in final form Aug. 1994

ABSTRACT

A laser source based on difference frequency generation (DFG) in $AgGaS_2$ has been developed for high resolution infrared kinetic spectroscopy of free radicals. Continuously tunable infrared radiation has been generated between 4 and 9 μm (2500-1100 cm^{-1}) by mixing two single frequency visible lasers in a 90° Type I phasematching configuration. To date, spectra of the free radicals HOCO, DOCO. and HCCN have been obtained using this source.

Concurrently, the suitability of III-V single-mode cw diode lasers for difference-frequency generation of tunable infrared radiation has been explored by mixing a red single-mode diode laser with a tunable single-mode cw $Ti:Al_2O_3$ laser in $AgGaS_2$. More than 1 μW of cw tunable, infrared ($\lambda \approx 5$ μm), narrow band coherent radiation has been generated by using type I noncritical phase-matching. The feasibility of a more compact, solid-state cw laser source based on the mixing of two single-mode diode lasers (808 and 690 nm) as pump sources in $AgGaS_2$ has also been demonstrated.

Techniques to increase the infrared difference-frequency output power level such as the use of a high-power optical semiconductor amplifier or an external buildup cavity for the nonlinear mixing

crystal have been investigated. As much as 47 μW of cw infrared radiation and 89 μW of pulsed infrared radiation, tunable around 4.3 μm have been generated by mixing the outputs of a high-power tapered semiconductor amplifier at 858 nm and a Ti:Al_2O_3 laser at 715 nm in $AgGaS_2$. recent progress in generating cw infrared radiation near 3.2 μm by mixing the outputs of an extended cavity diode laser near 800 nm and a compact diode-pumped Nd:YAG laser at 1064 nm in $AgGaS_2$ with an external enhancement cavity to resonate the signal wave inside the nonlinear mixing crystal is also described.

INTRODUCTION

There exists a need for continual improvement of convenient laser-based sources for high resolution spectroscopy. Since virtually all fundamental vibrational modes of molecules, free radicals, and molecular ions lie in the 2 to 20 μm wavelength region, tunable monochromatic sources in this range are particularly desirable. CW laser sources present the greatest potential for an optimum combination of spectral control and frequency stability. Although tunable cw laser sources such as color center lasers, lead-salt diode lasers, and CO and CO_2 sideband lasers emit in this spectral region, each type suffers from one or more practical drawbacks: the requirement of cryogenic cooling, operational wavelength ranges which do not reach regions of great interest, incomplete coverage of their nominal operational wave-length range, and lack of portability and ruggedness.

Difference frequency generation in a suitable nonlinear optical medium offers a viable alternative to traditional infrared laser sources, especially when wide tunability is desired. The DFG source originally developed by Pine [1] in which an Ar^+-laser is mixed with a cw dye laser in $LiNbO_3$ has proved very useful for high resolution spectroscopy but is limited to wavelengths shorter than 4 mm by the transmission characteristics of $LiNbO_3$. Using $LiIO_3$ as the nonlinear medium, Oka and coworkers extended the long wavelength limit for cw DFG spectroscopic sources to nearly 5 mm [2].

Advances in the development of nonlinear optical materials, such as $AgGaS_2$ and $AgGaSe_2$, now offer a convenient technique of generating cw tunable infrared narrow-band coherent radiation over a wide wavelength range (3 to 18 μm) by means of difference-frequency generation at room temperature. Recently, we demonstrated the operation of a continuously tunable cw DFG spectrometer

in the 4 to 9 μm (2400 to 1100 cm-1 region based on Type I 90° noncritical phasematching in a $AgGaS_2$ crystal pumped by two tunable single-frequency ring lasers [3,4]. This spectrometer extends the advantages of DFG sources into the chemically interesting "fingerprint" region of the IR, greatly increasing its applicability. This source is the essential element of an infrared kinetic spectroscopy apparatus designed to observe new free radicals. In the following we discuss the $AgGaS_2$ spectrometer; the observation of HOCO, DOCO, and HCCN; and experiments involving DFG in $AgGaS_2$ using III-V diode lasers as the pump and signal beam sources. The use of semiconductor diode lasers as pump sources in the nonlinear DFG mixing process is particularly attractive, as their compact size and ease of operation allow the construction of a portable and robust mid-infrared laser source.

EXPERIMENT

The $AgGaS_2$ DFG spectrometer, shown in Figure 1, has been described previously. (See Reference 4 for details). Two single frequency ring lasers, $d\lambda < 1$ MHz, were pumped by the all-lines output of an Ar^+ laser (Coherent Innova 200), typically operated at ~19 W. One ring laser (Coherent 899-21) operated in a dye cavity configuration lasing on DCM dye and generated the pump beam (λ = 620-690 nm). The second ring laser (Coherent 899-29) operating with a Ti:sapphire cavity configuration generated the signal beam (λ = 700-850 nm). The pump and signal laser polarizations were adjusted for 90° Type I ($e \rightarrow o + o$) phasematching by rotating the polarization of the Ti:saphire laser 90° and spatially overlapping the two beams with a polarization cube. The copropagating visible beams were focused into a 45 mm long $AgGaS_2$ crystal (Cleveland Crystals, Inc.) to a beam waist of ~40 μm. the infrared radiation generated in the crystal was collimated and propagated through a ZnSe beamsplitter. A portion of the IR light passed through a 20 cm reference gas cell and was monitored by a liquid nitrogen cooled HgCdTe detector. The other portion of the IR traversed a multipass absorption cell (White cell) with a base pathlength of 1 m and was monitored by a second HgCdTe detector. The excimer laser radiation used to create the transient radical population entered one end of the White cell, overlapped the IR, and was terminated in a beam trap at the opposite end. Germanium filters with antireflective IR coatings were placed in front of each HgCdTe detector to eliminate the residual visible and UV laser light.

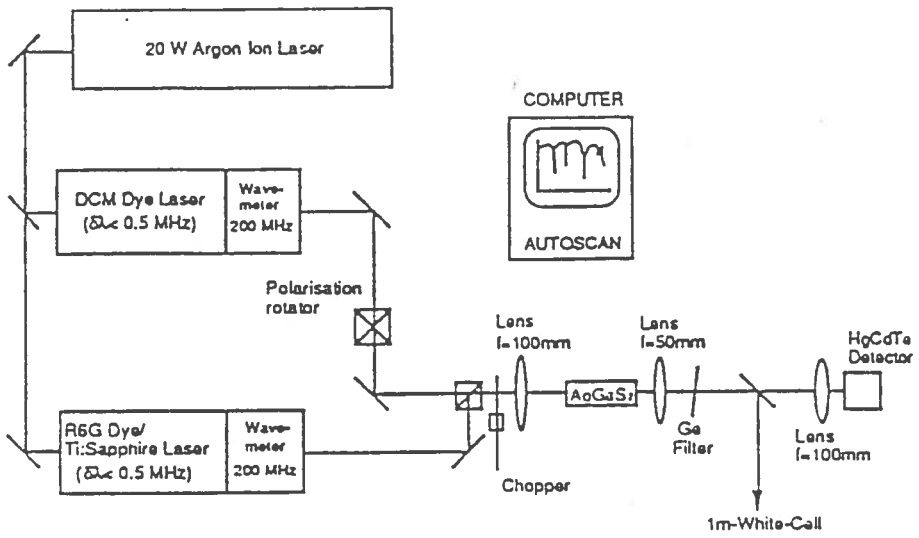

Fig. (1) Schematic of $AgGaS_2$ DFG Spectrometer

The 193 nm photolysis of acetic acid, CH_3COOH and CH_3COOD (98% D) produced HOCO and DOCO, respectively. HCCN was generated by the 193 nm photolysis of dibromoacetonitrile, Br_2HCCN. Precursor compounds were introduced into the White cell by gently bubbling He carrier gas through liquid samples. The sample gas mixture and additional He buffer gas flowed through the cell so that their steady-state pressures were typically 300 millitorr and 8 Torr, respectively. Gas samples were replenished between every excimer laser pulse. The White cell was adjusted for 24-32 passes, and there was an effective physical overlap of ~28 cm per pass in the middle of the cell.

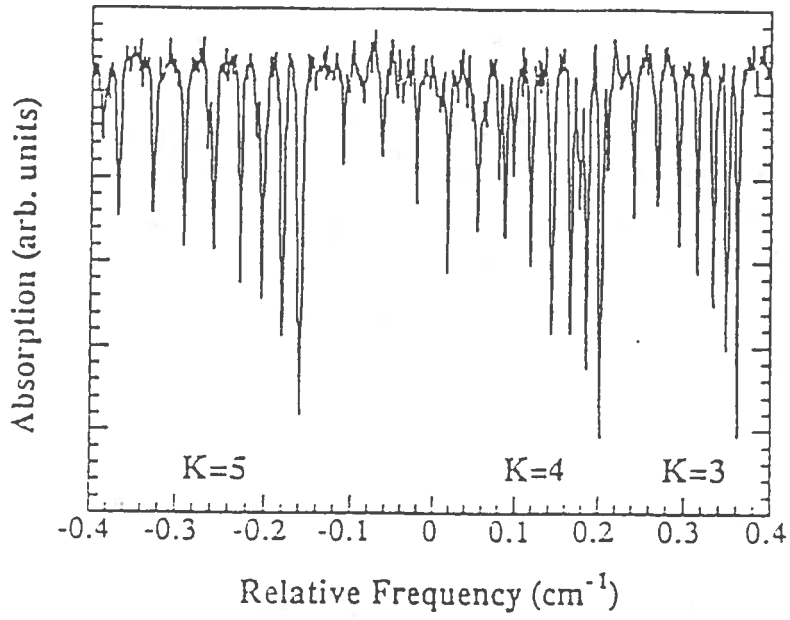

Fig. (2) HOCO ν_2 Q Branch near 1852 cm^{-1}

The DFG spectrometer provides the resolution and brightness necessary to investigate the infrared spectra and reaction dynamics of transient free radicals. To demonstrate the capabilities of the spectrometer, we reinvestigated the ν_2 C = O stretching spectra of HOCO and DOCO near 1860 cm^{-1} recently reported by Sears and coworkers. The spectra in Figures 2 and 3, showing portions of the HOCO and DOCO ν_2 Q branches, illustrate that Doppler limited resolution was achieved. Line positions and relative intensities are in excellent agreement with those recorded previously using lead salt diode lasers (5). Closer inspection suggests that the DFG spectra exhibit slightly better resolution characteristics than the diode laser spectra, even though Doppler broadening is the limiting factor in both cases.

Although we successfully observed the free radicals HOCO and DOCO, their spectroscopy was previously known. Therefore, we searched for the ν_2 CCN antisymmetric stretching mode spectrum of the HCCN radical. HCCN is especially interesting due to the debate over its equilibrium geometry. High level *ab initio* calculations indicate that the lowest energy structure has an HCC bond angle of 138°

(6,7), while virtually all experimental results favor a linear structure (8-10). The calculated barrier to linearity ranges from 300 to 800 cm^{-1} (6,7), suggesting a large amplitude HCC bending motion and possible quasi-linearity in this radical. Very recently, our group has observed the ν_1 CH stretching mode spectrum of this radical using the color center laser spectrometer (11) and found evidence for a small barrier to linearity (~100 cm^{-1}) based on the values for ν_4, ν_5, and $2\nu_5$ determined from various hot band series. The $\nu 2$ spectrum should be even more sensitive to the HCCN quasi-linearity, since the *ab initio* structure calculations indicate that the CCN antisymmetric stretching motion, CC bond compression, and CN bond elongation is strongly coupled to the bent-to-linear transformation (6,7).

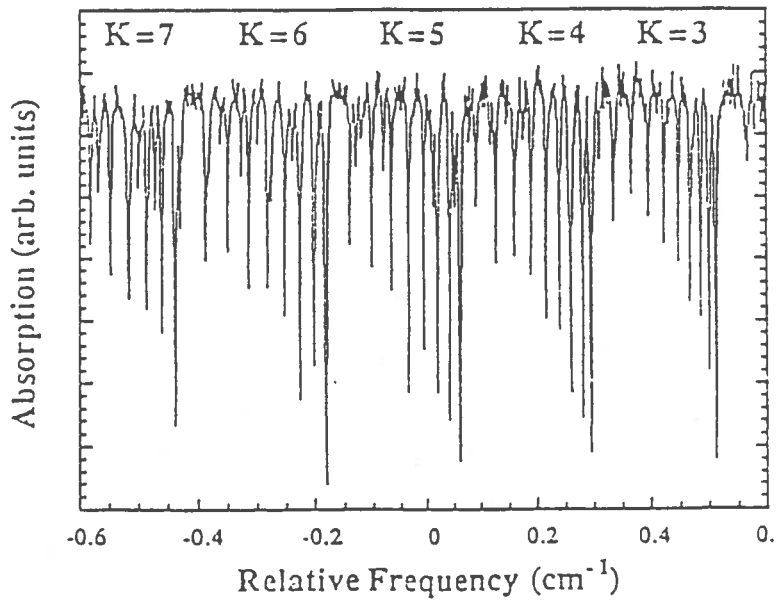

Fig. (3) DOCO ν_2 Q Branch near 1850 cm^{-1}

IR matrix studies (10) located the HCCN ν_2 transition at 1735 cm^{-1}. We scanned this area and found numerous transient absorption lines. Figure 4 shows a characteristic 3 cm^{-1} wide segment of this spectrum. HCCN lines were observed throughout the region between 1715 and 1765 cm^{-1}, but data

analysis has been hampered by the large number overlapping spectral series due to transitions originating from vibrational levels above the ground state.

DFG WITH III-V DIODE LASERS

Recent advances in high-power single-mode III-V diode laser technology (12) now offers the possibility of employing diode lasers as pump sources in DFG. Efficient, compact, robust, and portable spectrometers especially suitable for applications in selective environmental monitoring of trace species can be constructed using a diode laser based DFG source. Potentially, IR radiation from 3 to 6 μm by DFG in $AgGaS_2$ using Type I noncritical phasematching can be generated by mixing currently commercially available AlGaInP, AlGaAs, InGaAs, and/or InGaAsP III-V diode lasers (13).

In the development of a compact DFG spectrometer based on two single-mode diode lasers, we made use of the already existing DFG spectrometer (3.4). In a first step (14) a cw tunable $Ti:Al_2O_3$ ring laser operating in the wavelength range from 690 to 840 nm and a single-mode diode laser polarized for 90° Type I ($e \rightarrow o + o$) phasematching in $AgGaS_2$ were spatially overlapped with the polarizing beam splitter (Figure 1). The visible beams were focused into the 45 mm long. $AgGaS_2$ crystal to a beam waist of about 40 μm by using a 10 cm focal-length lens (as the diode laser beam is not a Gaussian beam, we define its "waist" as the half-width where the beam intensity is down by $1/e^2$). The infrared radiation generated in the mixing crystal was collimated with a 5 cm focal-length CaF_2 lens and detected after the germanium filter with a liquid-N_2 cooled photoconductive HgCdTe detector followed by a lock-in amplifier.

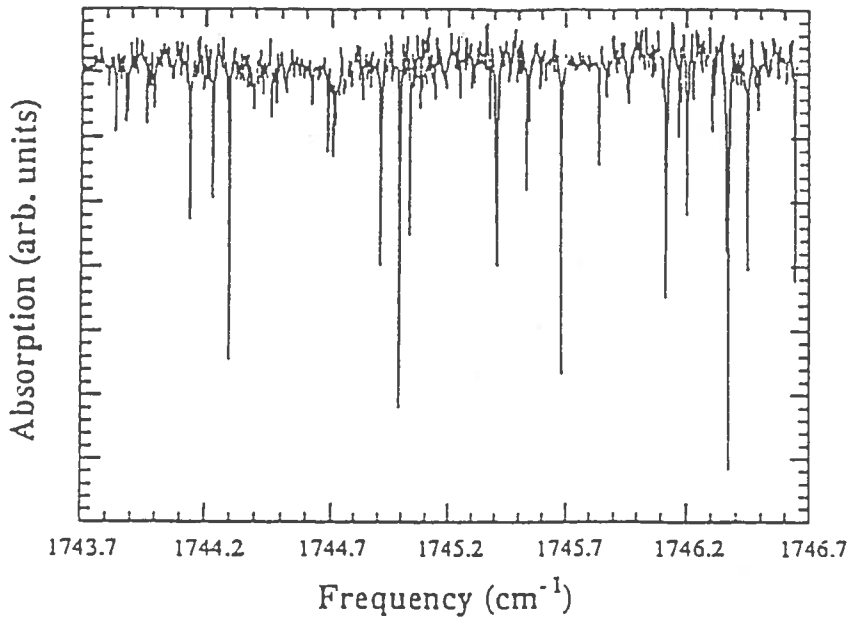

Fig. (4): A 3 cm^{-1} portion of HCCN ν_2 CCN antisymmetric stretching mode spectrum.

The three diode lasers used in this experiment were unmodified commercial devices operating at 671 nm, 690 nm, and 808 nm. Their spectral linewidths were measured to be 120 MHz, 30 MHz, and 90 MHz, respectively. Each was operated in a single longitudinal mode, so that both spontaneous background and extraneous modes were down by more than 25 dB from the dominant spectral mode. By varying the temperature and the current of the diodes, their emission wavelength could be tuned over about 2 nm. The collimated diode laser beam with a rectangular beam shape of 1x5 mm2 cross-section was converted to a square-shaped beam with a beam dimension of approximately 5 mm by using an anamorphic prism pair. A 3:1 telescope transformed the diode laser beam size to a dimension comparable to that of the Ti:Al2O3 laser. The spatial mode quality of each diode laser was characterized by passing it through an aperture and measuring the transmitted power.

The diode laser wavelengths were determined to within 0.5 nm by using an optical multi-channel analyzer consisting of a 0.32 m Czerny-Turner configuration monochromator with a photodiode array attached to the output slit plane of the monochromator. For a signal and pump wavelength of

808.3 nm ($Ti:Al_2O_3$ laser) and 690.3 nm (Toshiba TOLD 9140(s) diode laser), respectively, an idler wavelength of 4.73 μm was detected. For 1 W of $Ti:Al_2O_3$ laser power and 12.1 mW of diode laser power a DFG power of up to 1.4 μW were measured. The phase-matching bandwidth of the diode/$Ti:Al_2O_3$ pump laser configuration was observed to be as large as 600 GHz. This is much larger than the phase-matching bandwidth of about 30 GHz observed for the dye/$Ti:Al_2O_3$ pump laser configuration (3,4). Apparently, poor spatial coherence of the diode laser beam results in reduced power, but extended phase-matching range. The high resolution capability of this novel spectroscopic source was demonstrated by obtaining a Doppler-limited CO absorption spectrum around 2119 cm^{-1} using a 20 cm absorption cell and about 10 Torr of CO pressure (Figure 5). In this case the diode laser wavelength was fixed, and the infrared wavelength was changed by tuning the $Ti:Al_2O_3$ laser. The detector's NEP is 3.7. 10^{-10} W. However, the dominant source of noise in the spectrum was fluctuations of the generated infrared power level resulting from changes of the relative spatial overlap of the visible beam waists in the $AgGaS_2$ crystal due to mechanical instabilities of the experimental set-up.

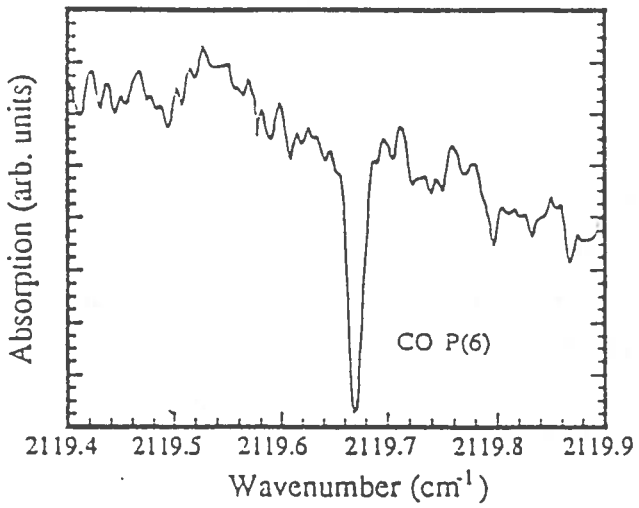

Fig. (5): CO absorption spectrum near 2119 cm^{-1} using a 20 cm absorption cell and about 10 Torr of CO pressure.

A laser diode (Toshiba TOLD 9215(s)), emitting up to 9 mW in a single mode at 671.4 nm, was phase-matched with the Ti:Al_2O_3 laser at 772.8 nm. For 5.2 mW diode laser power and 1.15 W Ti:Al_2O_3 laser power, the infrared power at 1963 cm^{-1} was ~1.2 μW. In order to investigate the effect of the non-Gaussian diode laser beam on the DFG conversion efficiency, the experiment was repeated using the DCM dye laser set to the same wavelength and power level as the diode laser. The infrared output of the dye/Ti:Al_2O_3 laser combination, like the diode/Ti:Al_2O_3 laser combination, showed a linear dependence of IR power upon the input signal power, but the slope was a factor of three greater. Thus, the non-Gaussian diode laser mode does not mix as effectively with the pure TEMoo Gaussian mode of the Ti:Al_2O_3 signal source, as does the pure TEMoo Gaussian mode from the dye laser.

The feasibility of mixing two single-mode diode lasers in $AgGaS_2$ to generate tunable infrared radiation was also demonstrated. The radiation from each diode laser was collimated and then converted to a square-shaped beam using anamorphic prism pairs. After being spatially overlapped with a polarizing beam splitter, the beams traversed a 3:1 telescope and were focused into the $AgGaS_2$ nonlinear crystal. Using a Toshiba TOLD 9140(s) diode laser and a Sharp LT010MD diode laser emitting at 690 nm and 808 nm with power levels of 10.1 mW and 1.93 mW, respectively, we were able to generate up to 3.3 nW of infrared radiation around 2115 cm^{-1}.

However, if KTP is used as the nonlinear optical DFG material, Wang and Ohtsu (15) recently generated as much as 300 nW near 1.6 μm from two diode lasers (50 mW each). Accounting for the different experimental conditions such as input power levels, input wave-lengths, crystal size, and effective nonlinear coefficient, the nonlinear conversion efficiencies of both all-diode-DFG experiments is on the same order of magnitude.

DFG WITH HIGH-POWER SEMICONDUCTOR OPTICAL AMPLIFIERS

One way to increase the DFG output power to a level that is useful for spectroscopic applications is the use of optical semiconductor amplifiers to boost the power output of the single-mode diode lasers. Significant progress has been made in obtaining diffraction-limited coherent radiation from high-power broad-area and array laser diodes (16,17) and, more recently, traveling-wave (TW)

amplifiers (18). When seeded by a single-stripe low-power master diode laser (18), the semiconductor amplifier has been demonstrated to generate near diffraction-limited, single-longitudinal mode emission required for applications such as nonlinear frequency conversion through second harmonic generation (19) or sum-frequency mixing (20). Under pulsed operation 11.6 W of peak power was generated by a broad-area amplifier seeded by a laser diode (18). High-power cw amplifier operation required for many applications has been considerably more difficult to achieve. Recently, however, 5.25 W of cw emission (21) was obtained from a tapered stripe (18,22) GaAlAs amplifier seeded with a Ti:Al_2O_3 laser.

We demonstrated difference-frequency mixing of a high-power GaAlAs tapered traveling-wave semiconductor amplifier (23) with a cw Ti:Al_2O_3 laser in a 45 mm long $AgGaS_2$ crystal cut for Type I noncritical phase-matching at room temperature. The experimental setup used in this work is shown in Figure 6. The master laser was index-guided diode laser (SDL Inc. Model SDL5410C), emitting up to 130 mW in a single-longitudinal mode around 860 nm with a less than 20 MHz linewidth. By changing the temperature, the laser wavelength was tunable over ~1-2 nm. The amplifier chip was bonded active side down on a heatsink which, in turn, was attached to a water cooled fixture and allowed unobstructed optical access to both facets. After collimation by a f=2.0 mm lens (0.5 NA), the master laser power passed though a Faraday solator, and a 3x beam expander. Final coupling of the injected signal into the amplifier was accomplished by a combination of a closely spaced f = 15 cm cylindrical lens and a high numerical aperture f = 7.7 mm lens. The cylindrical lens served to move the focused point of the input beam to several hundred μm in fron of the facet in the junction plane, while allowing it to coincide with the facet in the perpendicular plane (18). This highly astigmatic input resulted in a Gaussian input beam width of approximately 150 μm in the junction plane and 1 mm in the perpendicular plane. With 100 mW of master laser power incident on the amplifier, 38 mW was coupled into the amplifier. The GaAlAs tapered amplifier used in this work was characterized by a 250 μm input width, 500 μm output width, 1.5 mm length, and a single quantum well separate confinement heterostructure active region. At high currents the amplifier had a peak gain 860 nm. The facets of the amplifier were antireflection coated ($R \approx 10^{-3}$) at 860 nm for single-pass traveling-wave operation. A second f = 7.7 mm lens was used to collimate the amplifier emission perpendicular to the junction. In the junction plane the emission was brought to a focus by the f = 7.7 mm lens and collimated by a f = 10 cm cylindrical lens.

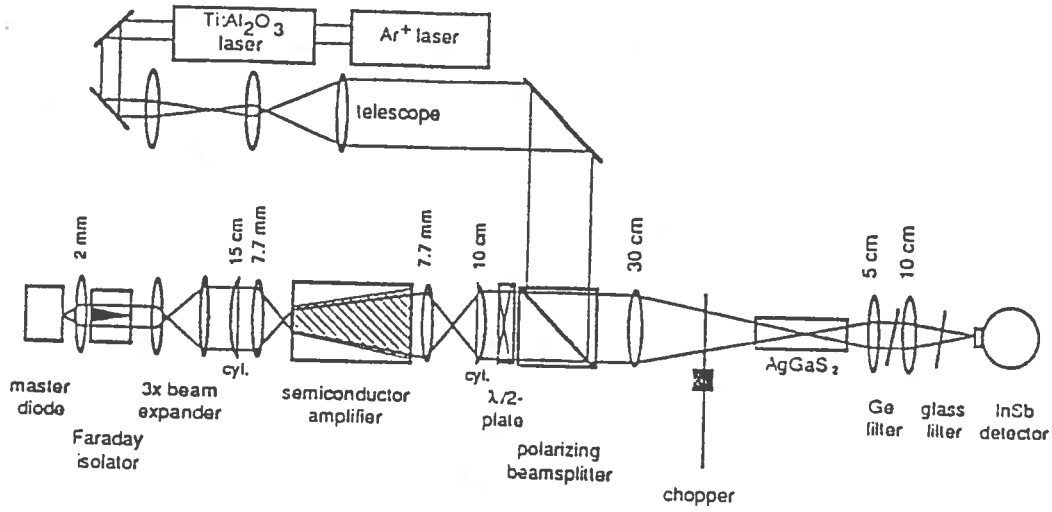

Fig. (6) DFG using of a high-power GaAlAs tapered traveling-wave semiconductor amplifier with a cw Ti:Al2O3 laser in a 45 mm long AgGaS crystal cut for Type I noncritical phase-matching at room temperature.

The pump wave was provided by a $Ti:Al_2O_3$ ring laser operated at 715 nm, close to its short-wavelength operation limit. In order to maximize the power output, the laser was operated multi-longitudinal mode without intracavity etalons, resulting in a linewidth of ~1 GHz. Pump and signal wave polarizations were chosen perpendicular to each other for 90° Type I phase-matching in $AgGaS_2$. Both beams were overlapped using a polarizing beam splitter and focused into the 45 mm long $AgGaS_2$ crystal using a 30 cm focal-length lens. A three-lens telescope design in the pump laser beam path allowed matching of beam waist widths and focal points for the two beams at the location corresponding to the center of the crystal. The beam waists were set to ~33 μm in both vertical and horizontal planes, close to optimum focusing (3). As measured with a scanning slit beam profiler, the spatial distribution of pump and signal beams was near-Gaussian, where in the case of the signal wave (amplifier) approximately 20% of the focused light was in sidelobes outside the main Gaussian envelope.

The amplifier output power incident on the nonlinear crystal was measured with an integrating sphere detector as a function of the amplifier current. A maximum signal wave power of 1.5 W was obtained under cw operation, and 3.2 W under pulsed operation with 50 ms long pulses and 0.1% duty cycle. After correcting for the 75% capture efficiency of the f = 7.7 mm lens and transmission losses of the beamsplitter and other optical components, the actual amplifier output at the maximum cw current of 6 A was 2.5 W. The maximum operating currents for the amplifier were arbitrarily chosen and do not represent a fundamental operating limit of the amplifier.

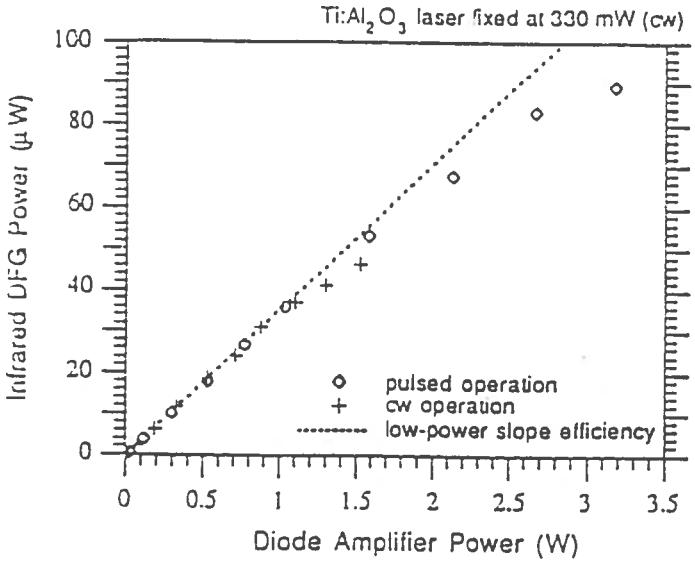

Fig. (7): Generated infrared DFG power as a function of the diode amplifier output power for cw and pulsed amplifier operation. The dotted line indicates the low-power external slope efficiency of ~35 μW/W for the DFG process.

The differences-frequency long wavelength radiation generated in the $AgGaS_2$ crystal was collimated with a 5 cm focal-length CaF_2 lens and focused on liquid N_2 cooled photovoltaic InSb detector with a sensitive area elements of 4 mm diameter (Graseby Infrared IS-4). An antireflection coated germanium filter was used to block pump and signal waves and pass the difference-frequency radiation. To avoid saturation of the detector-preamplifier combination at the highest powers obtained under pulsed amplifier operation, a glass filter (T = 2.8% at 4.3 μm) in front of the detector was used to attenuate the detector signal. Phase-matching was found to occur at a wavelength of 714.60 nm and 858.60 nm for pump and signal wave, respectively, corresponding to a generated difference-frequency wavelength of ~4.26 μm (2350 cm^{-1}). The laser wavelengths were determined with a spectral resolution of ~0.1 nm and an absolute spectral accuracy of ~0.1 nm using a multi-mode probe fiber connected to an optical spectrum analyzer (HP 70951 A Optical Spectrum Analyzer). The phase-matching bandwidth was observed to be on the order of the spectral resolution of the optical spectrum analyzer. Tuning of the infrared wavelength was limited to ~25 cm^{-1} by the limited temperature tuning range of the master diode laser.

Figure 7 shows the generated infrared DFG power as a function of the diode amplifier output power for cw and pulsed amplifier operation. Values shown are corrected for the 4.3 μm transmission loss of the optical components between the crystal and the detector, but not for the 17% Fresnel reflection at the crystal output facet. For all measurements the Ti:Al_2O_3 laser output was fixed at a cw power of ~330 mW, and the diode amplifier output power was changed by varying the pump current. The dotted line indicates the low-power external slope efficiency of ~35 μW/W for the DFG process. Maximum difference-frequency powers of 47 μW and 89 μW were obtained for the cw and pulsed operation, respectively (24). The drop in experimental slope efficiency at high amplifier power levels is attributed to the degradation in the diode laser beam quality occurring at highest amplifier currents. To evaluate the contribution of thermal effects in the mixing crystal to the drop in slope efficiency at high amplifier power levels, the absorption loss in the $AgGaS_2$ crystal was determined at the signal wavelength. From the ratio of transmitted to reflected signal power, we found the absorption in $AgGaS_2$ at 858 nm to be as low as ~0.091 to 0.015 cm^{-1}. At high signal power levels, no decay of the infrared pulse amplitude during the 50 ms pulse was observed, indicating that thermal lensing did not contribute to the drop in experimental slope efficiency occurring at the highest pulsed powers. Correction for the

Fresnel reflection losses for pump, signal, and idler waves at the surface of the uncoated $AgGaS_2$ crystal, the germanium filter, and the CaF_2 lenses results in an internal slope efficiency of ~65 μW/W at 330 mW cw $Ti:Al_2O_3$ pump power. No significant improvement in the slope efficiency was observed when changing the $Ti:Al_2O_3$ laser from multi-mode to single-mode operation by inserting the intracavity etalons into the ring laser cavity.

RESONANT ENHANCEMENT CAVITY SCHEME FOR DFG

Alternatively, the DFG conversion efficiency can be increased by making use of the high circulating fields present inside optical cavities by placing the nonlinear crystal either in an external (passive) enhancement cavity or in one of the pump laser cavities.

We are currently investigating the use of an external enhancement cavity built around the nonlinear optical $AgGaS_2$ crystal to resonate the signal wave, thereby increasing the signal power present inside the mixing crystal. As the infrared power generated in the nonlinear three-wave mixing process scales with the product of the signal and pump powers, enhancement of the signal power equally increases the nonlinear conversion efficiency. An extended cavity diode laser near 800 nm and a compact diode-pumped Nd:YAG laser at 1064 nm are used as the pump and signal sources of the difference-frequency generation (DFG) process, respectively.

Our passive DFG buildup cavity (Figure 8) used to resonate the 1064 nm signal wave is a modification of the four-mirror cavity used by Polzik and Kimble (25). It consists of three flat mirrors (M_1-M_3) and two lenses (f_{L1} = 25 mm, f_{L2} = 50 mm) together with a 5 mm long $AgGaS_2$ crystal cut for Type I noncritical phase-matching. The linear dimension of the cavity are ~25 cm with the total angle θ on mirror M_1 being 3^o. Both facets of the nonlinear optical mixing crystal are coated with a three-layer antireflection-coating for low loss at 1064 nm ($R \approx 4.10^{-5}$). In spite of the quality of coatings, passive losses from the lenses (R < 0.2% /surface) reduce the cavity buildup relative to bow-tie cavities with curved mirrors (26). However, the cavity setup shown in Figure 8 can be realized almost exclusively with standard Nd:YAG laser optics. Mirrors M_2 and M_3 are HR-coated (R > 99.7%) at 1064 nm. The infrared radiation generated inside the crystal is coupled out through M_2,

which was an Al_2O_3-substrate HR-coated (R > 99.7%) at 1064 with a transmission T≈70% at the generated difference-frequency of ~3 μm. M_1 is used as the input coupler with R≈ 96% at 1064 nm chosen to impedance-match (27) the buildup cavity to the driving signal power. Approximately 70% of the diode laser power at 795 nm incident on the cavity can be coupled in through M_1.

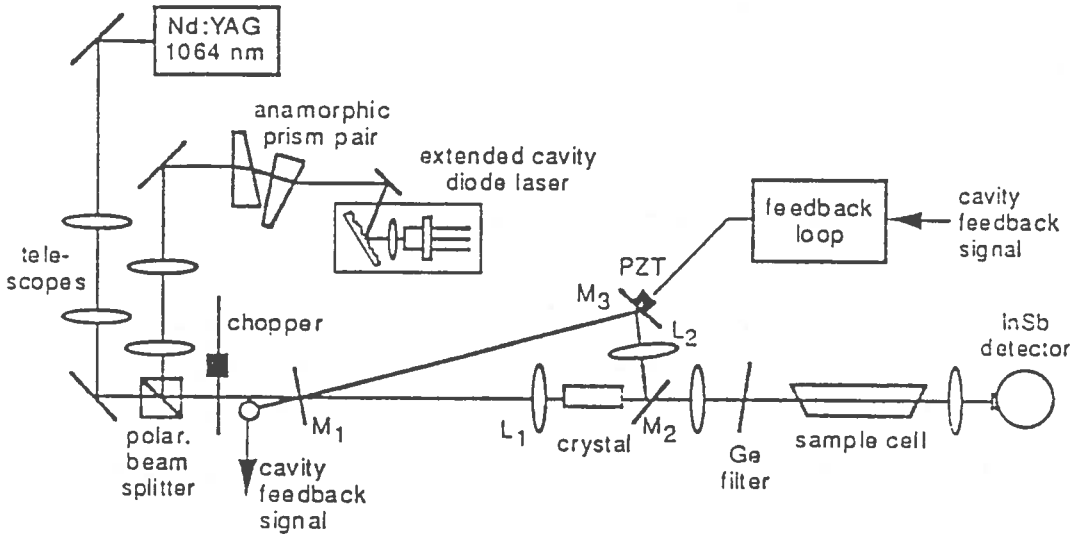

Fig. (8): Use of a 3-mirror external buildup cavity for the nonlinear crystal to increase the infrared DFG output power.

More than 1 μW of cw infrared radiation near 3.2 μm has been generated by difference-frequency mixing the outputs of a single-mode extended cavity semiconductor diode laser (pump source) near 795 nm and a diode-pumped Nd:YAG laser (signal source) in $AgGaS_2$ using Type I phase-matching (28). The signal source was resonated in a ring enhancement cavity resulting in buildup factors for the signal power of up to 15. The compact infrared DFG source could be tuned from 3.145 to 3.4 μm (3180-2930 cm^{-1}) and was used to detect the fundamental v_3-asymmetric stretching motion

of methane in direct and WM-absorption spectroscopy. Methane was chosen in this feasibility study because of its environmental significance (important greenhouse gas, supports ozone formation in polluted air). The performance of the demonstrated source can be further improved by using a lower loss buildup cavity (25).

CONCLUSIONS

In conclusion, DFG in $AgGaS_2$ utilizing diode/Ti:Al_2O_3 and diode/diode laser input configurations has been demonstrated, producing mid-infrared radiation.

As much as 47 μW of cw and 89 μW of pulsed infrared radiation around 4.3 μm have been generated by difference-frequency mixing the outputs of an injection-seeded GaAlAs tapered semiconductor amplifier and a Ti:Al_2O_3 laser in $AgGaS_2$ using Type I non-critical phase-matching. It is anticipated that the use of an external enhancement cavity for the nonlinear mixing crystal will also result in significantly improved DFG performance.

A wide range of applications such as chemical analysis, remote sensing, pollution detection, and medical research is anticipated for this new diode laser based tunable mid-infrared sensor technology.

ACKNOWLEDGMENTS

This work has been supported by the Robert A. Welch Foundation and the National Science Foundation. The authors would like to thank C.C. Bradley, R.F. Curl, R.G. Hulet, and C.E. Miller (Rice University, Houston, Texas); L. Goldberg (NRL, Washington, DC); and S. Waltman and L. Hollberg (NIST, Boulder, Colorado) for significant contributions. U. Simon gratefully acknowledges the support of the Alexander von Humboldt Foundation by a Feodor Lynen Fellowship.

REFERENCES

1. A.S. Pine, J. Opt. Soc. Am. 64, 1683 (1974).
2. M.G. Bawendi, B.D. Rehfuss, and T. Oka, J. Chem. Phys. 93, (1990) 6200; L.W. Xu, C. Gabrys, and T. Oka, J. Chem. Phys. 93, (1990) 6210.
3. P. Canarelli, Z. Benko, R.F. Curl, and F.K. Tittel, "continuous-Wave Infrared Laser Spectrometer Based on Difference Frequency Generation in $AgGaS_2$ for High-Resolution Spectroscopy," J. Opt. Soc. Am. B 9, (1992) 197.
4. A.H. Hielscher, C.E. Miller, D.C. Bayard, U. Simon, K.P. Smolka, R.F. Curl, and F.K. Tittel, "Optimization of a Mid-Infrared High Resolution Difference Frequency Spectrometer," J. Opt. Soc. Am. B 9, (1992) 1662.
5. T.J. Sears, W.M. Fawzy, and P.M. Johnson, J. Chem. Phys. 97, (1992) 3996.
6. P.A. Malmquist, R. Lindh, B.O. Roos, and S. Ross, Theor. Chim. Acta 73, (1988) 155.
7. E.T. Seidl and H.F. Schaefer, III, J. Chem. Phys. 96, (1992) 4449, and extensive experimental and theoretical references therein.
8. S. Saito, Y. Endo, and E. Hirota, J. Chem. Phys. 80, (1984) 1427.
9. F.X. Brown, S. Saito, and S. Yamamoto, J. Mol. Spectrosc. 143, (1990) 203.
10. A. Dendramis and G.E. Leroi, J. Chem. Phys. 66, (1977) 4334.
11. C.L. Morter, S.K. Farhat, and R.F. Curl, Chem. Phys. Lett. 207, (1993) 153
12. C.E. Wieman and L. Hollberg, Rev. Sci. Instrum. 62, (1991) 1.
13. K. Nakagawa, M. Ohutsu, C.H. Shin, M. Kourogi, and Y. Kikunaga, Laser Spectroscopy (Tenicols '91), M. Ducloy, ed. Singapore: World Scientific, (1992), pp. 353-358.
14. U. Simon, C.E. Miller, C.C. Bradley, R.G. Hulet, R.F. Curl, and F.K. Tittel, "Difference-Frequency Generation in $AgGaS_2$ by Using Single-Mode Diode Laser Pump Sources," Opt. Lett. 18, (1993) 1062.
15. W. Wang and M. Ohtsu, "Frequency-Tunable Sum- and Difference - Frequency Generation by Using Two Diode Lasers in a KTP Crystal," Opt. Common. 102, (1993) 304.
16. L. Goldberg and J.F. Weller, "Injection Locking and Single-Mode Fiber Coupling of a 40-Element Laser Diode Array," Appl. Phys. Lett. 50, (1987) 1713.

17. L. Goldberg and M.K. Chun, "Injection Locking Characteristics of a 1 W Broad Stripe Laser Diode," Appl. Phys. Lett. 53, (1988) 1900
18. L. Goldberg, D. Mehuys, M.R. Surette, and D.C. Hall, "High-Power, Near-Doffraction-L:imited Large-Area Traveling-Wave Semiconductor Amplifiers," IEEE J. Quantum Electron. QE-29, (1993) 2029.
19. L. Busse, L. Goldberg, and D. Mehuys, Electron. Lett. 29, (1993) 77.
20. L. Goldberg, M.K. Chun, I.N. Duling, III, and T.F. Carruthers, "Blue Light Generation by Nonlinear Mixing of Nd:YAG and GaAlAs Laser Emission in a $KNbO_3$ Rsonant Cavity," Appl. Phys. Lett. 56, (1990) 2071.
21. D. Mehugs, L. Goldberg, and D. Welch, "5.25-Watt Diffraction-Limited, Tapered Stripe Semiconductor Optical Amplifier," IEEE Photonics Tech. Lett. 5, (1993) 1179.
22. J.N. Walpole, E.S. Kintzer, S.R. Chinn, C.A. Wang, and L.J. Misaggia, "High-Power Strained-Layer InGaAs/AlGaAs Tapered Traveling Wave Amplifier," Appl. Phys. Lett. 61, (1992) 720.
23. F.J. Effenberger and G.J. Dixon, "2.95 mm Intracavity Difference-Frequency Laser", in Digest of Topical Meeting on Advanced Solid State Lasers Washington, DC: Optical Society of America, (1992), pp. 59.
24. U. Simon, F.K. Tittel, and L. Goldberg, "Difference-Frequency Mixing in AgGaS2 by Using a High-Power GaAlAs Tapered Semiconductor Amplifier at 860 nm," Opt. Lett. (1993) 18.
25. E.S. Polzik and H.J. Kimble, "Frequency Doubling with KNbO3 in an External Cavity," Opt. Lett. 16, (1991) 1400.
26. Z.Y. Ou, S.F. Pereira, E.S. Polzik, and H.J. Kimble, "85% Efficiency for CW Frequency Doubling from 1.08 to 0.54 mm," Opt. Lett. 17, (1992) 640.
27. W.J. Kozlovsky, C.D. Nabors, and R.L. Byer, "Efficient Second Harmonic Generation of a Diode-Laser Pumped CW Nd:YAG Laser Using Monolithic MgO:$LiNbO_3$ External Resonant Cavities," IEEE J. Quantum Electron. QE-24, (1988) 913.
28. U. Simon, S. Waltman, I. Loa, F.K. Tittel, and L. Hollberg, "External Cavity Difference Source in the Mid-Infrared Based on $AgGaS_2$ and Diode Lasers," submitted to JOSA B (1994).